

1-1-2013

Chaos and its control in semiconductor laser with delayed negative optoelectronic feedback

GUANG-YU JIANG

JUAN ZHANG

YAN HUANG

Follow this and additional works at: <https://journals.tubitak.gov.tr/physics>



Part of the [Physics Commons](#)

Recommended Citation

JIANG, GUANG-YU; ZHANG, JUAN; and HUANG, YAN (2013) "Chaos and its control in semiconductor laser with delayed negative optoelectronic feedback," *Turkish Journal of Physics*: Vol. 37: No. 3, Article 4.

<https://doi.org/10.3906/fiz-1209-12>

Available at: <https://journals.tubitak.gov.tr/physics/vol37/iss3/4>

This Article is brought to you for free and open access by TÜBİTAK Academic Journals. It has been accepted for inclusion in Turkish Journal of Physics by an authorized editor of TÜBİTAK Academic Journals. For more information, please contact academic.publications@tubitak.gov.tr.

Chaos and its control in semiconductor laser with delayed negative optoelectronic feedback

Guang-yu JIANG,^{1,*} Juan ZHANG,² Yan HUANG¹

¹Key Laboratory of Nondestructive Testing (Ministry of Education), Nanchang Hangkong University, Nanchang, P.R. China

²College of Management, Jiangxi City University, Nanchang, P.R. China

Received: 26.09.2012 • Accepted: 14.03.2013 • Published Online: 13.09.2013 • Printed: 07.10.2013

Abstract: We reveal theoretically chaos and its control in a semiconductor laser with delayed negative optoelectronic feedback. Under nonperiodic or sinusoidal period optoelectronic current, the semiconductor laser exhibits rich nonlinear dynamics. For a given coupling constant, chaos is shown in a semiconductor laser directly injected by external light. For a photoelectric delayed negative-feedback scheme with sinusoidal period optoelectronic current, the laser can be controlled in single-periodic, dual-periodic, multi-periodic states, and even chaos. The results also illustrate what we think to be a new method to generate various period states in the chaos system.

Key words: Semiconductor laser, chaos, negative feedback

1. Introduction

Since chaos synchronization was put forward first by Pecora and Carroll in 1990 [1], chaos and its control have attracted extensive attention. In particular, semiconductor lasers (SLs) subject to optical feedback, optoelectronic feedback, or optical injection can conveniently generate chaotic signal for its potential applications such as a feedback interferometer [2], secured communications [3], all-optical frequency conversion [4], laser chaos-based LiDAR [5], and radar and sensors [6,7]. The SL with optical feedback can be served as a good candidate for source generators of chaos secure communications because of generating high-dimensional broadband chaos and then ensuring a high level of security. Recently, many schemes of secure communications based on feedback-induced chaos in SLs have been proposed, and the systematical performances of synchronization and data communications have been investigated theoretically and experimentally. Very recently, nonlinear dynamics of SLs under repetitive optical pulse injection have been investigated numerically [8,9].

In this paper, we extend the systematical frame of [10–13] to the case of SLs under photoelectric delayed negative feedback in a chaos communication system. Under appropriate conditions, chaos and its control in a SL with delayed negative optoelectronic feedback have been investigated numerically and analytically. For different amplified control coefficients of optical currents, the rich dynamics, such as single-periodic, dual-periodic, multi-periodic, and chaos, are shown.

*Correspondence: jgy579@126.com

2. Model

The systematical configuration is depicted in Figure 1, where the solid lines and dashed lines indicate the electronic paths and the optical paths, respectively. The light output of an optically injected SL enters a beam splitter, which divides the SL output into 2 parts. One part is fed back into the SL through a photodetector (PD), optical controller (OC), and an amplifier (A) such that an optically injected SL is driven into chaos, and the other part is the output of the chaotic system.

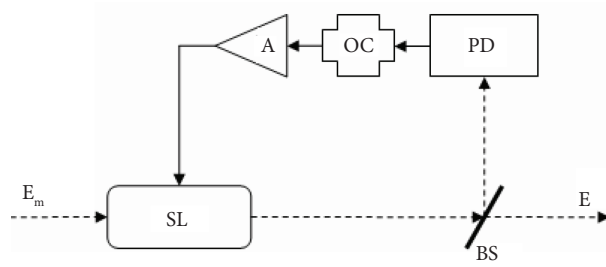


Figure 1. System configuration in semiconductor laser based on optoelectronic negative feedback. SL: semiconductor laser; BS: beam splitter; PD: photodetector; A: amplifier; OC: optical controller.

Our present study is based on a set of following modified rate equations including the laser fields E , the phases ϕ , and the carrier number N in the active region. This system can be theoretically described by [14,15]:

$$\frac{dE}{dt} = \frac{1}{2}(G - \nu_p)E + \frac{k \cdot E_m}{\tau_l} \cos(-\phi), \quad (1)$$

$$\frac{d\phi}{dt} = \frac{1}{2}\beta_c(G - \nu_p) + \frac{k}{\tau_l} \frac{E_m}{E} \sin(-\phi) - \Delta\omega_m, \quad (2)$$

$$\frac{dN}{dt} = \frac{I[1 - \rho E^2(t - \tau)/E_u^2]}{q} - \nu_e N - GV_p E^2, \quad (3)$$

where E and ϕ are the slowly varying electric field and phase of the laser optical field, respectively. N is the carrier number in the laser cavity. τ is the delayed time. E^2 is the laser intensity. E_u^2 is the output average power without control. ρ is the amplified control coefficient of the optical current. $G(= (\Delta\nu_g \alpha / V) (N - N_{th}) / \sqrt{1 + E^2/E_s^2})$ is the mode gain, ν_g is the laser cavity photon group velocity, α is the gain constant, ($= V/V_p$) is the compression and confinement factor, V is the volume of the laser cavity, V_p is the volume of the laser mode, and E_s is the saturation photon field strength. $N_{th} = n_{th}V$ is the carrier number at transparency and n_{th} is the carrier density at transparency. $\nu_p = \nu_g(\alpha_m + \alpha_{int})$ is the cavity decay rate of the photon, α_m is the external photon decay of the cavity, and α_{int} is the internal photon decay of cavity. $\Delta\omega_m$ is the detuning of the angular frequency between the master and slave lasers. $\tau_l = 2n_g L/c$ is the optical round-trip time in the laser cavity length of L , c is the vacuum speed of light, and $n_g = c/\nu_g$ is the group velocity refractive index. I is the drive current and q is the electronic charge. β_c is the line-width enhancement factor. $\nu_e = A_{nr} + B(N/V) + C(N/V)^2$ is the nonlinear decay rate of the carrier, A_{nr} is the nonradiative recombination rate, B is the radiative recombination factor, and C is the auger recombination factor. k is the optical injection coefficient.

In the system, the chaos and its control are realized by adopting a sinusoidal period current. Due to the presence of the sinusoidal period current, the periodic control term in Eq. (3) can be described as:

$$\frac{dN}{dt} = \frac{I\{1 - \rho[1 + A \cdot \sin(2\pi Mt)]E^2(t - \tau)/E_u^2\}}{q} - \nu_e N - GV_p E^2, \quad (4)$$

where A and M are the modulation depth and frequency, respectively.

3. Results and discussion

The rate equations given in Eqs. (1)–(4) can be numerically solved by the fourth-order Runge–Kutta method. The other parameters used in the calculation are chosen as [16,17]:

$L = 350 \mu\text{m}$, $w = 2 \mu\text{m}$, $d = 0.15 \mu\text{m}$, $\Gamma = 0.29$, $n_g = 3.8$, $\alpha_m = 29 \text{ cm}^{-1}$, $\alpha_{int} = 20 \text{ cm}^{-1}$, $\Delta\omega_m = 2\pi \times 10^9 \text{ rad/s}$, $\beta_c = 6$, $E_m = 0.126 \text{ Es}$, $n_{th} = 1.2 \times 10^{18} \text{ m}^{-3}$, $A_{nr} = 1 \times 10^{18} \text{ s}^{-1}$, $B = 1.2 \times 10^{-10} \text{ cm}^3 \text{ s}^{-1}$, $C = 3.5 \times 10^{-29} \text{ cm}^6 \text{ s}^{-1}$, $I = 25 \text{ mA}$, $E_s = 1.6619 \times 10^{11} \text{ m}^{-3/2}$, $\alpha = 2.3 \times 10^{-16} \text{ cm}^2$.

Figure 2 shows the time series and phase diagram in a SL without feedback. From this diagram, we can clearly see that when the SL is modulated directly from the external laser and the feedback coefficient ρ is set to be zero, the output dynamics is chaotic for a given coupling constant ($k = 0.05$) and the output average power is high.

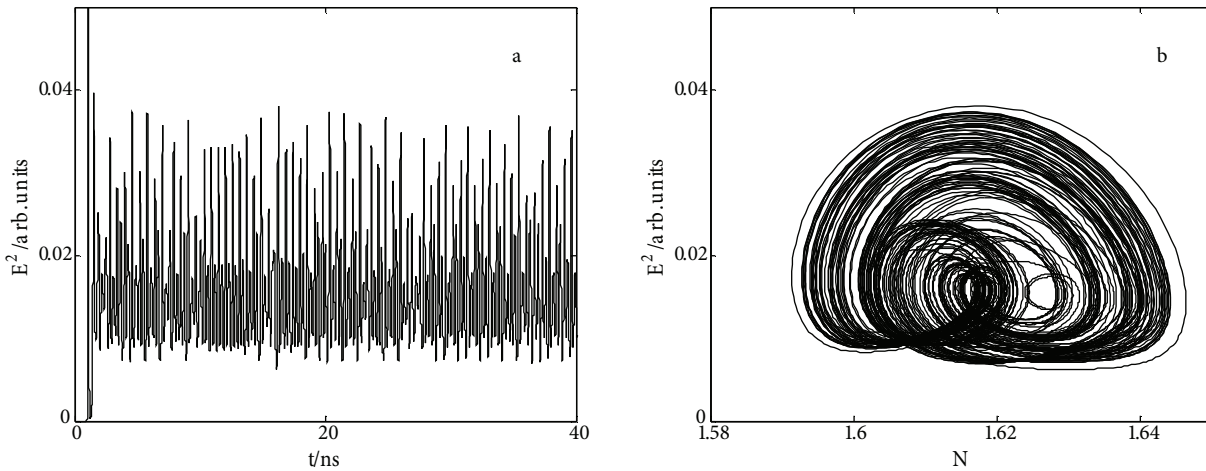


Figure 2. Time series and phase diagram for SL without delayed photoelectric negative feedback.

In the present of photoelectric delayed negative feedback, the injected SL presents rich dynamics for different control coefficients. When the coupling constant k is 0.05, the time series and phase diagram for the amplified control coefficient of the optical current ($\rho = 0.3$) are as shown in Figures 3a and 3b. It is clear that the SL is controlled to period 10 from the time series and the phase diagram, which are similar to the case of nonlinear states in the laser system in [12]. To further verify the nonlinear dynamics, we numerically calculate the rate equations of Eqs. (1)–(4) to obtain another multi-period state; the corresponding time series and phase diagram are presented in Figures 3c and 3d. When the coupling constant and delay time remain unchanged, the SL shows a multi-period state for a smaller amplified control coefficient of the optical current ($\rho = 0.2$). In addition, the pulse power gradually increases with the worsening of the amplified control coefficient of the optical current. The results show that the SL can be controlled much more easily, and the system shows more

nonlinear dynamics under photoelectric delayed negative feedback. Therefore, the laser system can be adjusted and controlled in a large parameter range and the laser shows a period state, a multi-period state, and chaos for the amplified control coefficient of the optical current, while its output average power is higher for a smaller control coefficient of the optical current.

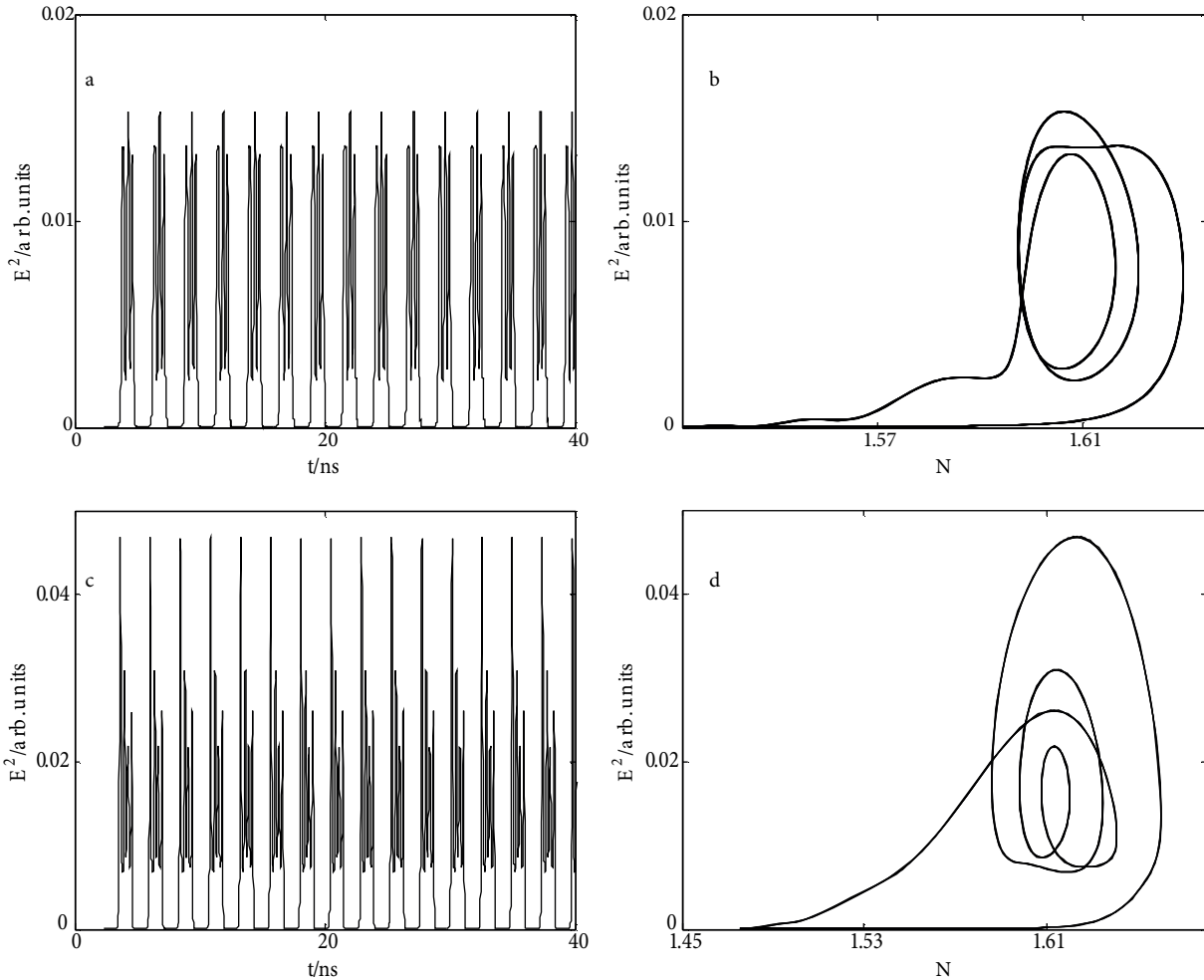


Figure 3. Time series (a, c) and phase diagrams (b, d) for SL with different feedback coefficients for a given coupling constant ($k = 0.05$).

In order to control and achieve more rich cycle states, the parameters of the SL are very important. Therefore, it is necessary to investigate the effect of parameters on chaos and its control in this scheme. We concentrate on the dynamics versus the different delay times for given sinusoidal period currents' parameters ($A = 0.5$, $M = 2$ GHz), which are described in Eq. (4). Figures 4 and 5 show the time series and phase diagram of the output dynamics versus different delayed times. As τ is 0.6 ns, the system is a suppressed 1-cycle for the amplified control coefficient of the optical current ($\rho = 0.1$), as shown in Figures 4a and 4b; the results show that when ρ is increased, the SL takes on another 1-period state and the orbit of the phase diagram changes in a nonobvious manner. As ρ is increased further to 0.5, the time series and phase diagram still show 1 period. However, when ρ is larger than 0.5, the SL shows more nonlinear dynamics. Here we select the delay time ($\tau = 1.3$ ns) with the 2-cycle controlled for the amplified control coefficient of the optical current ($\rho =$

0.2) in the system shown in Figures 4c and 4d. With increase of ρ , the SL takes on another 1-period state and the orbit of the phase diagram changes in a nonobvious manner. As ρ is increased further to 0.55, the time series and phase diagram still show 1 period. However, when ρ is larger than 0.55, the SL shows a chaos state. Its output average power changes in an unapparent way. The results indicate that the system with photoelectric delayed negative feedback and additive photoelectric delayed control easily realizes all types of the 1-cycle or 2-cycle states by adjusting the different delay times at the sinusoidal period currents' parameters.

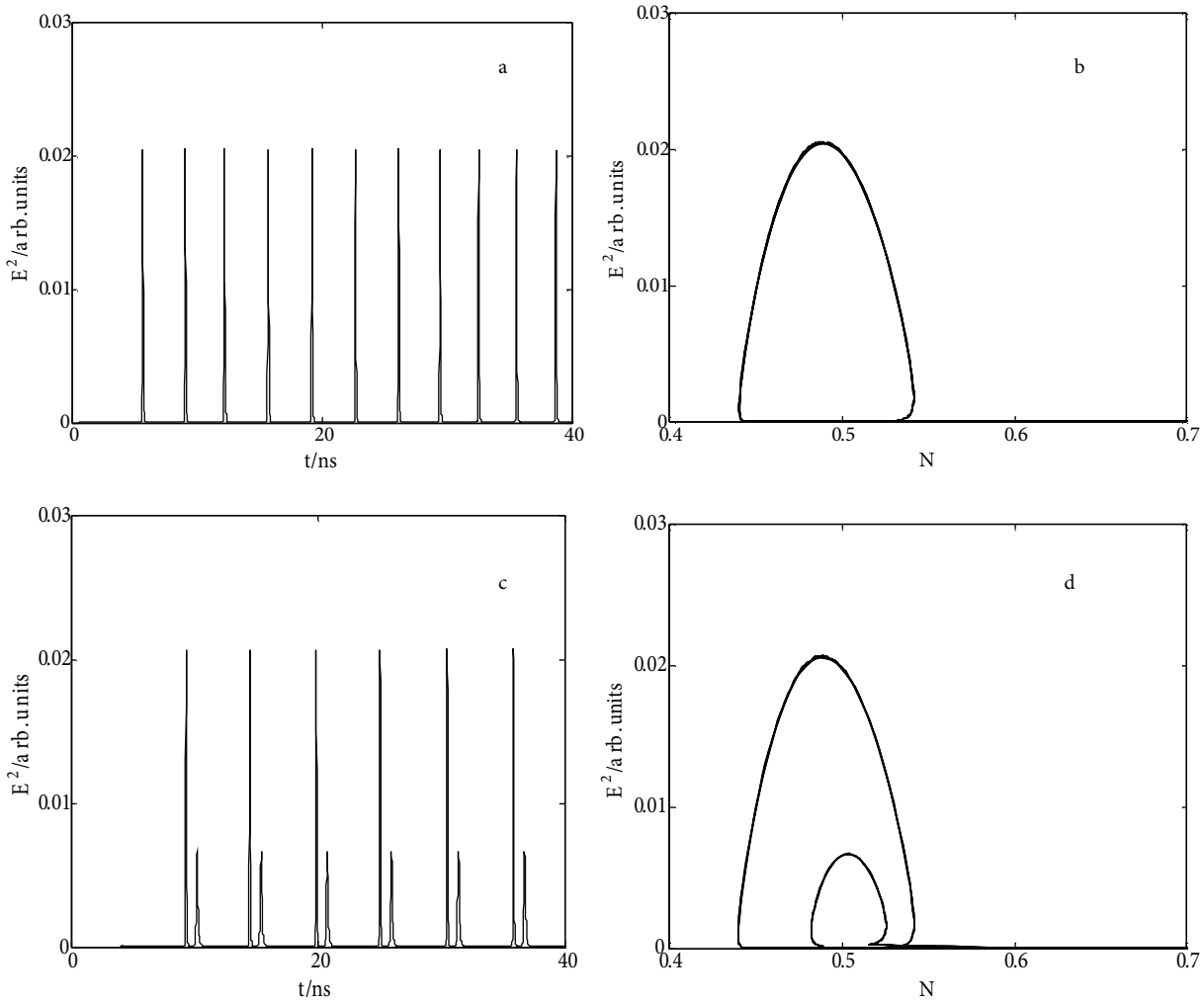


Figure 4. Time series (a, c) and phase diagram (b, d) for SL with different delay times and coefficients of optical current for given sinusoidal period currents' parameters ($A = 0.5$, $M = 2$ GHz).

To show other nonlinear dynamics, we select the delay time ($\tau = 1$ ns) for the SL showing a multi-period state and chaos. Figures 5a and 5b present the time series and phase correlation diagram of the output of SLs for the coupling constant ($k = 0.05$). For these diagrams, we find that the time series and phase portrait show multi-cycle states for a given amplified control coefficient of the optical current ($\rho = 0.1$). As ρ is increased, the SL takes on another multi-period state and the orbit of the phase diagram changes in a nonobvious manner. As ρ is increased further to 0.6, the time series and phase diagram still show a multi-cycle; when ρ is larger than 0.6, the SL shows more nonlinear dynamics. For the delay time ($\tau = 1.1$ ns),

the SL also shows multi-cycles for given amplified control coefficient of optical currents. Compared with the previous results, Figures 5c and 5d present time series and the phase correlation diagram of the output of SLs for the delay time ($\tau = 1.5 \text{ ns}$) at the same modulation depth and frequency ($A = 0.5$, $M = 2 \text{ GHz}$). The time series and phase portrait show chaos, and the pulse power changes apparently. Figure 6a shows the variation of normalized intensity versus different coupling constants for other given certain parameters. With the increase of the coupling constant, the laser is controlled in rich nonlinear dynamics. In Figure 6b, when the coupling constant is 0.05, the variation of normalized intensity changes with different feedback coefficients. We can see here that the laser can be successfully controlled in different periodic states. The results show that there are different ranges of delay times and control coefficients of the optical current, which can provide us with different dynamical behaviors. In addition, the system has a larger space of parameters. Therefore, by choosing appropriate delays and amplified control coefficients of the optical current, we can use the method of photoelectric delayed negative feedback and photoelectric delayed negative feedback with additive photoelectric delayed control for achieving chaos and its control.

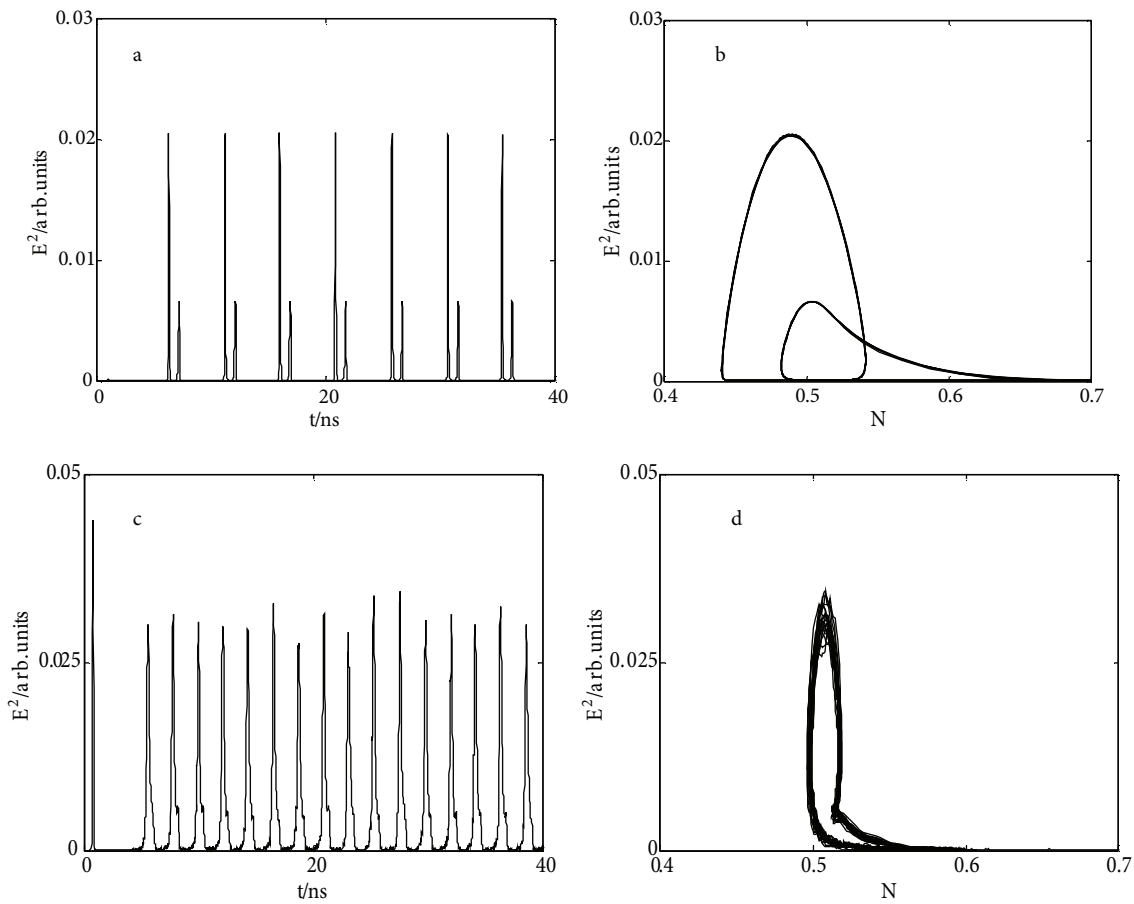


Figure 5. Time series (a, c) and phase diagrams (b, d) for SL with different delay times for given sinusoidal period currents' parameters and coefficients of optical current ($A = 0.5$, $M = 2 \text{ GHz}$, $\rho = 0.1$).

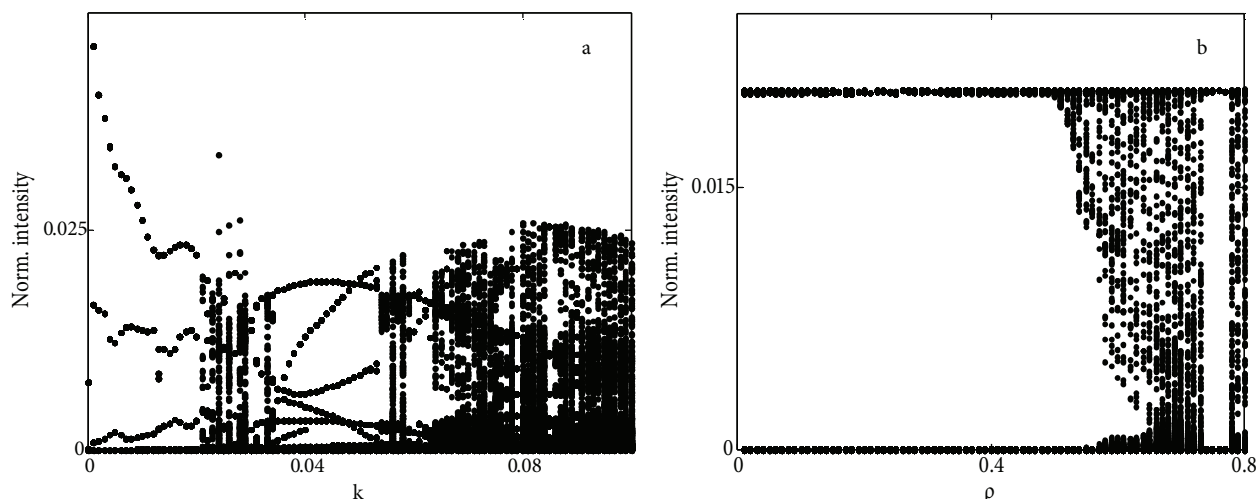


Figure 6. The variation of normalized intensity versus different coupling constants (a) and different feedback coefficients (b).

4. Conclusions

We have presented a physical method to realize chaos and its control in an injected SL with delayed negative optoelectronic feedback. Under the action of the directly injection and nonperiodic and sinusoidal period current, the SL shows abundant nonlinear dynamics. The results show that chaos can be controlled and achieved easily, and this method can effectively achieve a laser system with a 1-cycle state, multi-cycle states, and chaos. Our investigation reveals that the delayed negative feedback coefficients, coupling constant, and control coefficients of optical current play an important role in the process of chaos and its control. We hope this work will offer useful insight to the nonlinear dynamics of chaotic laser systems.

Acknowledgments

This work was funded by the Foundation of the Jiangxi Education Bureau (GJJ10192) and the Foundation of the Key Laboratory of Nondestructive Testing (Ministry of Education) of China (ZD200929001).

References

- [1] Pecora, L. M.; Carroll, T. L. *Phys Rev. Lett.* **1990**, *64*, 821–824.
- [2] Pizolato, J. C.; Romero, M. A.; Goncalves Neto, L. *IEEE* **2008**, *55*, 1108–1115.
- [3] Tan, Y.; He, X. T.; Chen, S. G. *Chin. Phys. Lett.* **1993**, *10*, 321–324.
- [4] Hwang, C. C.; Hsieh, J. Y.; Lin, R. S. *Chaos Soliton. Fract.* **1997**, *8*, 1507–1515.
- [5] Tong, P. Q. *Acta Phys. Sin.* **1995**, *44*, 169–176.
- [6] Sato, M.; Aogaki, R. *Electrochimica Acta* **1995**, *40*, 2921–2925.
- [7] Hirasawa, K.; Murata, J.; Hu, J.; Jin, C. *IEEE* **2000**, *30*, 95–104.
- [8] Jiang, G. Y.; Zhang, J. *J. Optoelectron. Adv. Mater.* **2011**, *13*, 547–553.
- [9] Fu, Y. J.; Wang, W.; Jiang, G. Y. *J. Optoelectron. Adv. Mater.* **2011**, *13*, 348–353.
- [10] Layeghi, H.; Arjmand, M. T.; Salarieh, H.; Alasty, A. *Chaos Soliton. Fract.* **2008**, *37*, 1125–1135.
- [11] Uchida, A.; Sato, T.; Ogawa, T.; Kannari, F. *IEEE* **1999**, *35*, 1374–1381.

- [12] Yan, S. L. *Acta Phys. Sin.* **2008**, *57*, 2100–2106.
- [13] Rajesh, S.; Nandakumaran, V. M. *Phys. Lett. A.* **2003**, *319*, 340–347.
- [14] Zou, E.; Li, X. F.; Zhang, T. S. *Comp. Eng. Appl.* **2002**, *11*, 53–57.
- [15] Liu, Y.; Davis, P.; Takiguchi, Y.; Aida, T.; Saito, S.; Liu, J. M. *IEEE* **2003**, *39*, 269–278.
- [16] Tang, S.; Liu, J. M. *IEEE* **2003**, *39*, 1468–1475.
- [17] Wu, L.; Zhu, S. Q. *Chin. Phys.* **2003**, *12*, 300–304.